Free-field theory, fixed-point theory, and electron-positron annihilation into hadrons

D. K. Choudhury and A. K. Misra
Department of Physics, University of Gauhati, Gauhati 781014, Assam, India
(Received 28 January 1983)

The R problem of electron-positron physics is analyzed within the frameworks of a free-field theory (parton models) and a field theory with an infrared-stable fixed point. Present data do not rule out either of these models and hence they both can survive as alternatives to standard QCD in the R problem.

I. INTRODUCTION

The R problem of electron-positron annihilation has received considerable attention during recent years.[1] Most of the authors in recent times have studied it within the framework of QCD.[2–7] Here, we address ourselves to this problem within the frameworks of a free-field theory (or equivalently parton models) and a field theory with an infrared-stable fixed point. The R problem was studied earlier within these two approaches[8–10] before the discovery of new particles[11–13] and was found to be consistent with CEA and SPEAR data.[14–17] It is therefore tempting to restudy the problem using the present high-energy e^+e^- data[1,18] and to check whether these two approaches can be accommodated or ruled out. Thus the present analysis will check if existing scaling models of R other than standard QCD can survive in the present high-energy e^+e^- data.

In Sec. II, we discuss the problem within the context of a free-field theory, while Sec. III is devoted to a similar analysis with a field theory with an infrared-stable fixed point. Section IV contains comments and conclusions.

II. FREE-FIELD THEORY

A. Five-quark model

In the standard five-quark model with u,d,s,c,b quarks of masses m_u,m_a,m_s,m_c,m_b and three varieties of color, one has

$$R=3\left[\tfrac{2}{3}+\theta(s-s_{0\psi})\frac{4}{9}\left[1+\frac{2m_c^2}{s}\right]\left[1-\frac{4m_c^2}{s}\right]^{1/2}+\theta(s-s_{0\Upsilon})\frac{1}{9}\left[1+\frac{2m_b^2}{s}\right]\left[1-\frac{4m_b^2}{s}\right]^{1/2}\right]. \quad (2.1)$$

Here s is the (c.m. energy)^2 and $\sqrt{s_{0\psi}}\simeq 3.1$ GeV and $\sqrt{s_{0\Upsilon}}\simeq 9.1$ GeV corresponding to Ψ and Υ thresholds.

From experimental values of R,

$$R=3.0\pm 0.25 \text{ at } \sqrt{s}=4 \text{ GeV} (s_{0\Psi}<s<s_{0\Upsilon}),$$
$$R=3.66\pm 0.5 \text{ at } \sqrt{s}=27.5 \text{ GeV } (s>s_{0\Upsilon}), \quad (2.2)$$

we get

$$m_c=1.68\pm 0.03 \text{ GeV}, \quad m_b=4.95\pm 1.24 \text{ GeV}, \quad (2.3)$$

which are quite consistent with the estimates by Barnett *et al.*[7] Here and below, we have taken the calculated error to be equal to

$$[(\text{statistical error})^2+(\text{systematic error})^2]^{1/2}.$$

In Fig. 1, we draw the R-W plot of Eq. (2.1) where $W=\sqrt{s}$.

In Eq. (2.1), we have neglected light-quark masses (m_u,m_d,m_s). Giving them a common value m_L, Eq. (2.1)

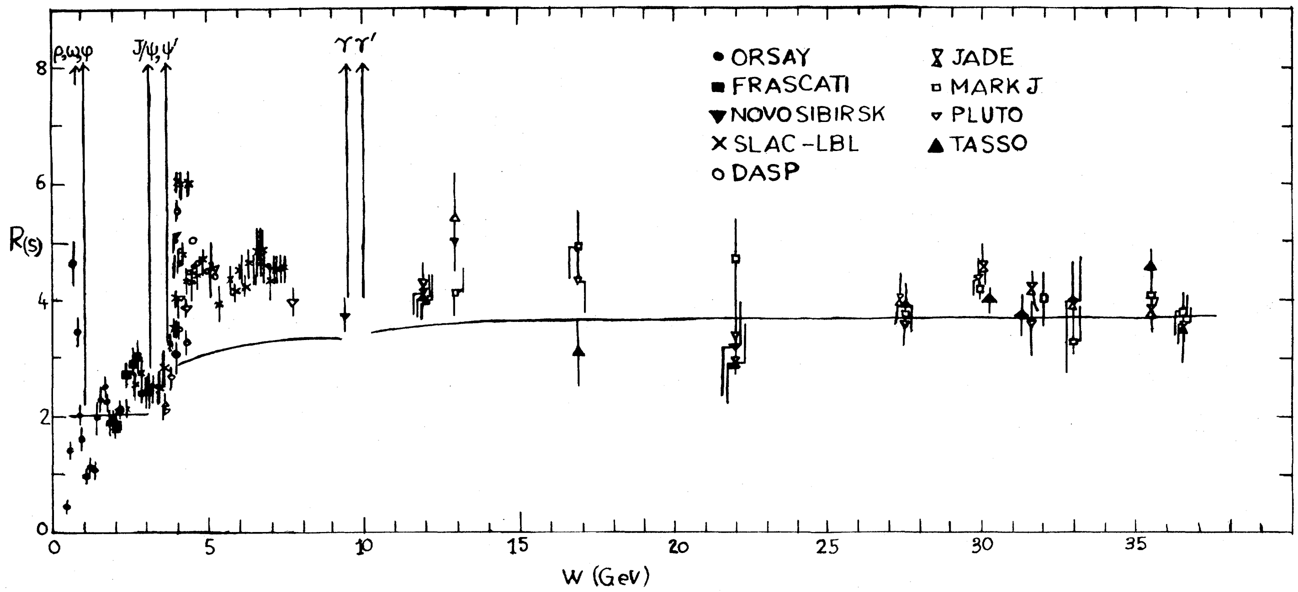

FIG. 1. $R(s)$ vs W with a five-quark model with $m_L=0$.

is modified to

$$R=\left[\frac{2}{3}\left[1+\frac{2m_L{}^2}{s}\right]\left[1-\frac{4m_L{}^2}{s}\right]^{1/2}+\theta(s-s_{0\Psi})\frac{4}{9}\left[1+\frac{2m_c{}^2}{s}\right]\left[1-\frac{4m_c{}^2}{s}\right]^{1/2}\right.$$
$$\left.+\theta(s-s_{0\Upsilon})\frac{1}{9}\left[1+\frac{2m_b{}^2}{s}\right]\left[1-\frac{4m_b{}^2}{s}\right]^{1/2}\right]. \quad (2.4)$$

From the experimental input[1,18]

$$R_1=1.95\pm0.2 \text{ at } \sqrt{s_1}=2 \text{ GeV } (s_1<s_{0\Psi},s_{0\Upsilon}),$$
$$R_2=3.0\pm0.25 \text{ at } \sqrt{s_2}=4 \text{ GeV } (s_{0\Psi}<s_s<s_{0\Upsilon}),$$
$$R_3=3.66\pm0.5 \text{ at } \sqrt{s_3}=27.5 \text{ GeV } (s_3>s_{0\Upsilon}), \quad (2.5)$$

we get

$$m_L=0.48\pm0.1 \text{ GeV},$$
$$m_c=1.68\pm0.1 \text{ GeV}, \quad (2.6)$$
$$m_b=5.08\pm1.23 \text{ GeV}.$$

The corresponding R-W plot is shown in Fig. 2.

From Figs. 1 and 2, we see that the standard five-quark model is in overall agreement with the mean experimental data. However, we note that a significant fraction of data in the continuum region is scattered away from the prediction of the model.

B. General free-quark model

Let us now consider a general free-field theory over and above the specific parton model discussed above. For this purpose, we consider a parton model with quarks of masses $m_1,\dots,m_n$ having charges $Q_1,\dots,Q_n$ with a color group $SU_c(l)$.

The most general formula for R in a free-parton model is

$$R=l\sum_{i=1}^{n}Q_i{}^2\left[1+\frac{2m_i{}^2}{s}\right]\left[1-\frac{4m_i{}^2}{s}\right]^{1/2}\times\theta(s-s_{0i}), \quad (2.7)$$

where s_{0i}'s are the thresholds associated with quarks Q_i's. We can make phenomenological use of (2.7), without specifying the values of $Q_1,\dots,Q_n$, $m_1,\dots,m_n$, and l, if we make a free-quark expansion with a few nonleading terms above all thresholds ($s\gg s_{0i}$'s). This is due to the reason that Eq. (2.7) contains unspecified number of quark parameters (mass, charge, color) and only a free-quark expansion can reduce the number of parameters to the order of the expansion to be discussed below.

C. Free-quark expansion

Expanding Eq. (2.7) up to second, third, and fourth order, respectively, one has

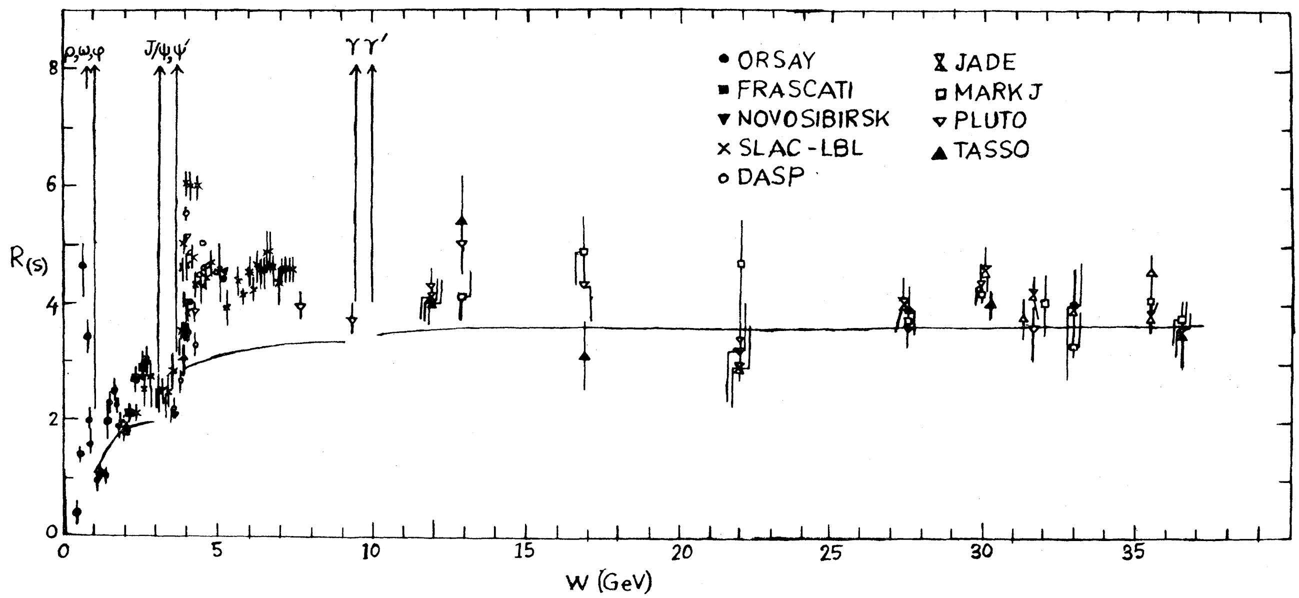

FIG. 2. $R(s)$ vs W with a five-quark model with $m_L \neq 0$.

$$R_{\mathrm{II}}(s)=R_{\infty}\left[1-\frac{6x}{s^2}\right], \tag{2.8}$$

$$R_{\mathrm{III}}(s)=R_{\infty}\left[1-\frac{6x}{s^2}-\frac{6y}{s^3}\right], \tag{2.9}$$

$$R_{\mathrm{IV}}(s)=R_{\infty}\left[1-\frac{6x}{s^2}-\frac{6y}{s^3}-\frac{6z}{s^4}\right]. \tag{2.10}$$

Here

$$x=\frac{\sum Q_i^2 m_i^4}{\sum Q_i^2}, \tag{2.11}$$

$$y=\frac{4}{3}\frac{\sum Q_i^2 m_i^6}{\sum Q_i^2}, \tag{2.12}$$

$$z=3\frac{\sum Q_i^2 m_i^8}{\sum Q_i^2}, \tag{2.13}$$

and

$$R_{\infty}=l\sum_i^n Q_i^2 . \tag{2.14}$$

Equations (2.8)–(2.10) show that in a free-field theory the approach to asymptopic behavior is a power law in s and from below [i.e., $R(s_1)>R(s_2)$ for $s_1>s_2$].[8,9] This behavior is to be contrasted with that of QCD, where the approach to the limiting value of R is from above [i.e., $R(s_1)<R(s_2)$ for $s_1>s_2$] and logarithmic in s, since[2–7]

$$R=R_{\infty}\left[1+\frac{b}{\ln(s/\mu^2)}\right] \tag{2.15}$$

with $b>0$. In Eq. (2.15) we have neglected terms $O(1/s^2)$ (which are common to a parton model and QCD) compared with the logarithmic one.

We now use Eqs. (2.8)–(2.10) for the high-energy R data above the experimental thresholds and find best fits with these three forms. To use above the Υ threshold, we recast Eqs. (2.8)–(2.10) in the forms

$$R_{\mathrm{II}}(s)=R_{\infty}\left[1-6\tilde{x}\left[\frac{m_{\Upsilon}^2}{s}\right]^2\right], \tag{2.16}$$

$$R_{\mathrm{III}}(s)=R_{\infty}\left[1=6\tilde{x}\left[\frac{m_{\Upsilon}^2}{s}\right]^2-6\tilde{y}\left[\frac{m_{\Upsilon}^2}{s}\right]^3\right], \tag{2.17}$$

$$R_{\mathrm{IV}}(s)=R_{\infty}\left[1-6\tilde{x}\left[\frac{m_{\Upsilon}^2}{s}\right]^2-6\tilde{y}\left[\frac{m_{\Upsilon}^2}{s}\right] -6\tilde{z}\left[\frac{m_{\Upsilon}^2}{s}\right]^4\right] \tag{2.18}$$

with

$$\tilde{x}=\frac{x}{m_{\Upsilon}^4}, \quad \tilde{y}=\frac{y}{m_{\Upsilon}^6}, \quad \tilde{z}=\frac{z}{m_{\Upsilon}^8}. \tag{2.19}$$

Here $\tilde{x},\tilde{y},\tilde{z}$ are dimensionless quantities and m_{Υ} is the mass of the Υ particle $m_{\Upsilon}=9.1$ GeV. We now record our main results.

(a) Analysis with Eq. (2.16). Using[1,18]

$$R(s_1)=4.0\pm0.44 \text{ at } \sqrt{s_1}=30.4 \text{ GeV}\,,\qquad R(s_2)=3.9\pm0.56 \text{ at } \sqrt{s_2}=27.5 \text{ GeV}\,, \tag{2.20}$$

we obtain the best fit with

$$R_\infty=4.2\pm0.19\,, \tag{2.21}$$

$$\tilde{x}=0.42\pm0.32 \tag{2.22}$$

in the continuum region above the Υ threshold.

(b) Analysis with Eq. (2.17). Using[1,18]

$$R(s_1)4.0\pm0.44 \text{ at } \sqrt{s_1}=30.4 \text{ GeV}\,, \tag{2.23}$$

$$R(s_2)=3.9\pm0.56 \text{ at } \sqrt{s_2}=27.5 \text{ GeV}\,, \tag{2.24}$$

$$R(s_3)=3.4\pm0.8 \text{ at } \sqrt{s_3}=22 \text{ GeV}\,, \tag{2.25}$$

we obtain the best fit with

$$R_\infty=4.2\pm0.06\,, \tag{2.26}$$

$$\tilde{x}=0.83\pm0.01\,, \tag{2.27}$$

$$\tilde{y}=2.88\pm0.88\,. \tag{2.28}$$

(c) Analysis with Eq. (2.18). Using[1,18]

$$R(s_1)=4.1\pm0.51 \text{ at } \sqrt{s_1}=31.6 \text{ GeV}\,,\quad R(s_2)=4.0\pm0.44 \text{ at } \sqrt{s_2}=30.4 \text{ GeV}\,,\quad R(s_3)=3.9\pm0.56 \text{ at } \sqrt{s_3}=27.5 \text{ GeV}\,,\quad R(s_4)=3.4\pm0.8 \text{ at } \sqrt{s_4}=22 \text{ GeV}\,, \tag{2.29}$$

we obtain the best fit with

$$R_\infty=4.4\pm1.1\,, \tag{2.30}$$

$$\tilde{x}=1.36\pm0.18\,, \tag{2.31}$$

$$\tilde{y}=0.97\pm0.31\,, \tag{2.32}$$

$$\tilde{z}=1.17\times10^2\pm0.22\times10^2\,. \tag{2.33}$$

The R-W plot using Eqs. (2.16), (2.17), and (2.18) is shown in Fig. 3. Our result shows that the present formalism can explain the continuum data of R in the high-energy end suggesting that the free-quark expansion cannot be extrapolated down to the Υ threshold. It also suggests the asymptotic limit of R to be $R_\infty \gtrsim 4.0-4.4$, to be compared with the QCD limit of $R_\infty=\frac{11}{3}$. We can also make an estimate of (c.m. energy)^2 where R would be saturated. Let this saturation (energy)^2 be defined as $\tilde{s}_\infty$. Then using Eq. (2.16), R will reach its 99% saturation point at s_∞ defined to be

$$\frac{99}{100}=1-6\tilde{x}\left[\frac{m_\Upsilon{}^2}{s_\infty}\right]^2. \tag{2.34}$$

Using Eq. (2.22) we find the 99% saturation (energy)^2 to be

$$s_\infty=2028 \text{ GeV}^2 \tag{2.35}$$

or

$$\sqrt{s_\infty}=45.03 \text{ GeV}\,. \tag{2.36}$$

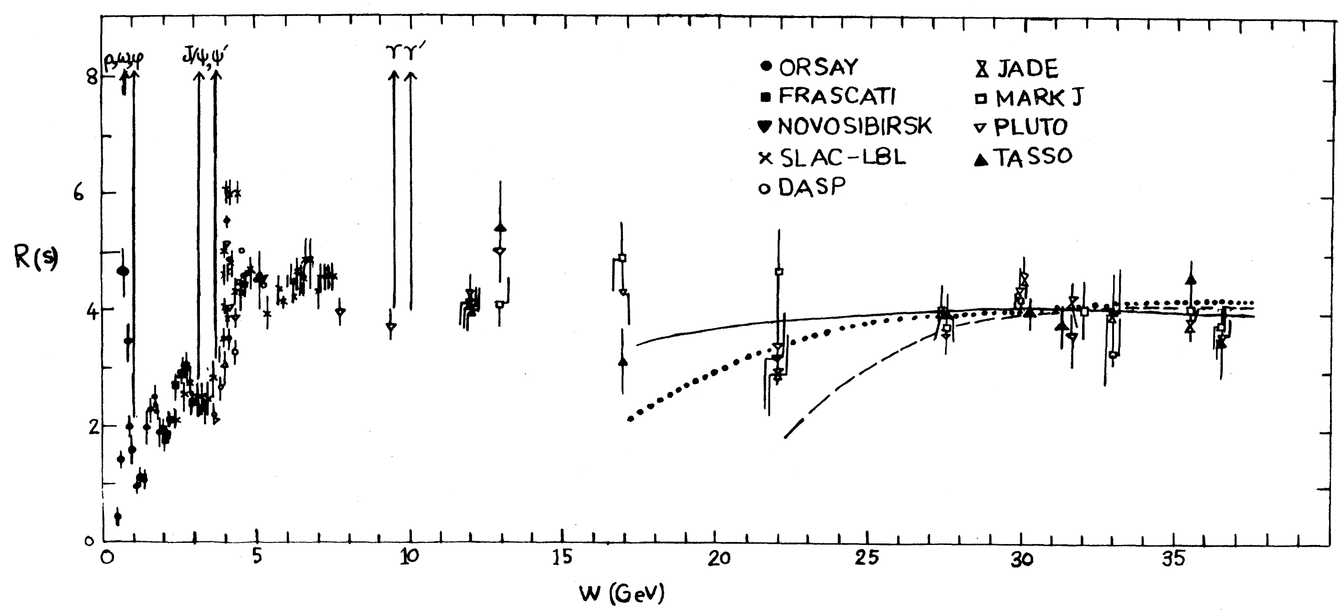

FIG. 3. $R(s)$ vs W with a free-quark expansion. Solid, dotted, and dashed curves correspond to expansions $O(1/s^2)$, $O(1/s^3)$, and $O(1/s^4)$, respectively.

Similar analysis of Eqs. (2.17) and (2.18), respectively, yields 99% saturation energy at $\sqrt{s_\infty}=44.2$ GeV and $\sqrt{s_\infty}=49.8$ GeV, respectively. We note that the present PETRA energy is limited to 40.5 GeV[1].

D. Positivity analysis with free-quark expansion

Further phenomenological application of Eq. (2.7) can be obtained if we use the truncated expressions (2.8)—(2.10) or (2.16)—(2.18) to determine the allowed domain of R_∞ from the positivity constraints of x,y,z (or equivalently $\tilde{x}$, $\tilde{y}$, $\tilde{z}$).[8,9] We note that all $(\text{mass})^2$ and $(\text{charge})^2$ are positive, x,y,z are necessarily positive. The advantage of this approach lies in the fact that it can accommodate more data in the continuum region within a general free-field hypothesis, Eq. (2.7).

Let us first consider Eq. (2.8). Let $R(s_1)$ be an experimental value of R at $s=s_1$. One then has

$$x=\frac{s_1^2}{6}\left[1-\frac{R(s_1)}{R_\infty}\right]. \tag{2.37}$$

Positivity of x here implies the trivial inequality

$$R_\infty > R(s_1) . \tag{2.38}$$

We now demonstrate that in the third-order case, Eq. (2.9), the condition that x and y are positive will constrain R_∞ in a nontrivial allowed domain. To see this let $R(s_1)$ and $R(s_2)$ be two different experimental values of $R(s)$ such that $s_1>s_2$. One then has

$$x=\frac{1}{6R_\infty(s_1-s_2)}\{R_\infty(s_1^3-s_2^3) -[R(s_1)S_1^3-R(s_2)S_2^3]\} , \tag{2.39}$$

$$y=\frac{s_1s_2}{6R_\infty(s_1-s_2}\{-R_\infty(s_1^2-s_2^2) +[R(s_1)s_1^2-R(s_2)s_2^2]\} . \tag{2.40}$$

Positivity of x yields

$$\infty \geq R_\infty \geq \frac{R(s_1)s_1^3-R(s_2)s_2^3}{s_1^3-s_2^3} , \tag{2.41}$$

while that of y yields

$$0 \leq R_\infty \leq \frac{R(s_1)S_1^2-R(s_2)s_2^2}{s_1^2-s_2^2} . \tag{2.42}$$

Thus, the allowed region of R_∞ is given by

$$\frac{R(s_1)s_1^3-R(s_2)s_2^3}{s_1^3-s_2^3} \leq R_\infty \leq \frac{R(s_1)s_1^2-R(s_2)s_2^2}{s_1^2-s_2^2} \tag{2.43}$$

for fixed $R(s_1)$, $R(s_2)$, s_1, and s_2.

Let us now demonstrate that in the fourth-order case, Eq. (2.10), if x, y, and z are positive, then R_∞ has also restrictive allowed domains. Let $R(s_1)$, $R(s_2)$, and $R(s_3)$ be three experimental values of $R(s)$, such that $s_1>s_2>s_3$. We then obtain the following expressions for x, y, and z:

$$x=\frac{1}{6R_\infty |s|}(R_\infty d_1-n_1) , \tag{2.44}$$

$$y=\frac{1}{6R_\infty |s|}(-R_\infty d_2+n_2) , \tag{2.45}$$

$$z=\frac{s_1s_2s_3}{6R_\infty |s|}(R_\infty d_3-n_3) , \tag{2.46}$$

where

$$|s|=(s_1-s_2)(s_2-s_3)(s_1-s_3) , \tag{2.47}$$

$$n_1=R(s_1)S_1^4(s_2-s_3)-R(s_2)s_2^4(s_1-s_3) +R(s_3)s_3^4(s_1-s_2) , \tag{2.48}$$

$$d_1=s_1^4(s_2-s_3)-s_2^4(s_1-s_3)+s_3^4(s_1-s_2) , \tag{2.49}$$

$$n_2=R(s_1)s_1^4(s_2^2-s_3^2)-R(s_2)s_2^4(s_1^2-s_3^2) +R(s_3)s_3^4(s_1^2-s_2^2) , \tag{2.50}$$

$$d_2=s_1^4(s_2^2-s_3^2)-s_2^4(s_1^2-s_3^2)+s_3^4(s_1^2-s_2^2) , \tag{2.51}$$

$$n_3=R(s_1)s_1^3(s_2-s_3)-R(s_2)s_2^3(s_1-s_3) +R(s_3)s_3^3(s_1-s_2) , \tag{2.52}$$

$$d_3=s_1^3(s_2-s_3)-s_2^3(s_1-s_3)+s_3^3(s_1-s_2) . \tag{2.53}$$

From Eqs. (2.44)—(2.53) we observe that x, y, and z will be positive if only (n_1,d_1), (n_2,d_2), and (n_3,d_3) satisfy certain conditions discussed below.

(a) Constraints from positivity of x. Case 1. If $R(s_1)$, $R(s_2)$, $R(s_3)$ and s_1, s_2, s_3 are such that $n_1>0$, $d_1>0$, then positivity of x yields

$$\infty \geq R_\infty \geq \frac{n_1}{d_1} . \tag{2.54}$$

Case 2. If $n_1<0$, $d_1<0$, then positivity of x yields

$$\infty \leq R_\infty \leq \frac{|n_1|}{|d_1|} . \tag{2.55}$$

Case 3. If $d_1 < 0$, $n_1 > 0$, then x cannot be positive.

Case 4. If $d_1 > 0$, $n_1 < 0$, then positivity of x cannot give any nontrivial constraints on R_∞.

(b) Constraints from positivity of y. Case 1. If $d_2 > 0$, $n_2 > 0$, then positivity of y yields

$$0 \le R_\infty \le \frac{n_2}{d_2} . \tag{2.56}$$

Case 2. If $d_2 < 0$, $n_2 < 0$, then positivity of y gives

$$\infty > R_\infty \ge \frac{|n_2|}{|d_2|} . \tag{2.57}$$

Case 3. For $d_2 < 0$, $n_2 > 0$, positivity of y cannot yield any nontrivial constraints of R_∞.

Case 4. For $d_2 > 0$, $n_2 < 0$, y cannot be positive.

(c) Constraints from positivity of z. Case 1. If $d_3 > 0$, $n_3 > 0$, then positivity of z yields

$$\infty > R_\infty \ge \frac{n_3}{d_3} . \tag{2.58}$$

Case 2. If $n_3 < 0$, $d_3 < 0$, then positivity of z yields

$$0 \le R_\infty \le \frac{|n_3|}{|d_3|} . \tag{2.59}$$

Case 3. For $d_3 < 0$, $n_3 > 0$, z cannot be positive.

Case 4. For $d_3 > 0$, $n_3 < 0$, there are no nontrivial bounds on R_∞ from positivity of z.

Let us now discuss our main numerical results from the present formalism.

(i) Positivity analysis with Eq. (2.17). We take experimental input[1,18]

$$R(s_1) = 4.0 \pm 0.44 \quad \text{at } \sqrt{s_1} = 30.4 \text{ GeV} ,$$
$$R(s_2) = 3.9 \pm 0.56 \quad \text{at } \sqrt{s_2} = 27.5 \text{ GeV} , \tag{2.60}$$

which yields, using Eqs. (2.39)—(2.43),

$$4.12 \pm 0.3 \le R_\infty \le 4.2 \pm 0.2 , \tag{2.61}$$

$$0.02 \le \tilde{x} \le 0.19 , \tag{2.62}$$

$$5.79 \le \tilde{y} \le 6.13 . \tag{2.63}$$

(ii) Positivity analysis with Eq. (2.18). We take experimental input[1,18]

$$R(s_1) = 4.0 \pm 0.44 \quad \text{at } \sqrt{s_1} = 30.4 \text{ GeV} , \tag{2.64}$$

$$R(s_2) = 3.9 \pm 0.56 \quad \text{at } \sqrt{s_2} = 27.5 \text{ GeV} , \tag{2.65}$$

$$R(s_3) = 3.2 \pm 0.8 \quad \text{at } \sqrt{s_3} = 22 \text{ GeV} , \tag{2.66}$$

which yields, using Eqs. (2.44)—(2.59),

$$4.11 \pm 0.21 \le R_\infty \le 4.14 \pm 0.2 , \tag{2.67}$$

$$0.22 \le \tilde{x} \le 0.23 , \tag{2.68}$$

$$0.6 \le \tilde{y} \le 4.4 , \tag{2.69}$$

$$9.9 \le \tilde{z} \le 40.1 . \tag{2.70}$$

In Fig. 4 we plot the positivity domains of the $R(S)$-W with Eqs. (2.17) and (2.18). Comparing with Fig. 3, we observe that the present analysis can accommodate more data in the high-energy end of R within a general free-field hypothesis [Eq. (2.7)].

We also note that 99% saturation of R_∞ occurs

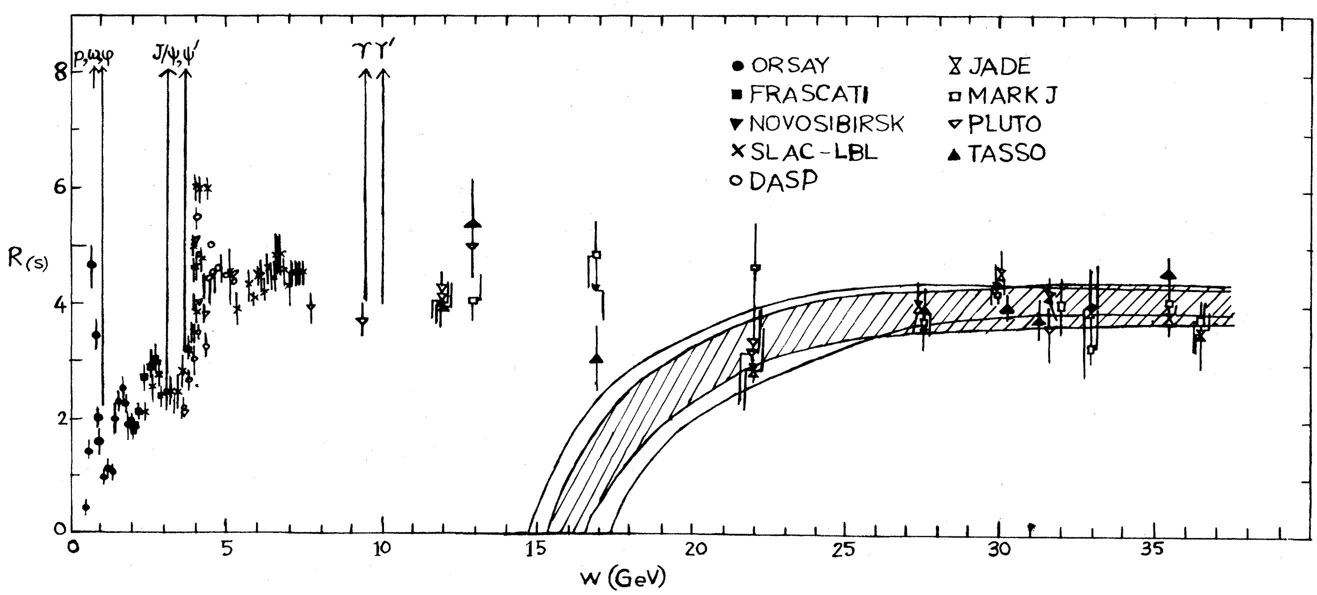

FIG. 4. Positivity domains of $R(s)$ vs W. The dashed and undashed domains correspond to the expansion $O(1/s^3)$ and $O(1/s^4)$, respectively.

in the (c.m.) energy $\sqrt{s_\infty}$:

$$\sqrt{s_\infty} \simeq 42.02 \text{ GeV} , \tag{2.71}$$

$$\sqrt{s_\infty} \simeq 39.6 \text{ GeV} , \tag{2.72}$$

using expansion up to third- and fourth-order terms, respectively.

III. R IN A FIELD THEORY WITH AN INFRARED-STABLE FIXED POINT

Some time ago, Wilson[19] had proposed that the strong interaction at short distances might be governed by a nontrivial infrared-stable fixed point of the renormalization group. Subsequently, Nachtmann[10] has shown that in such a field theory, $R(s)$ has a form given by

$$R(s) = R_\infty - \frac{B}{s^{(4-d\theta/2}} . \tag{3.1}$$

Here, d_θ is the dimension of θ, the trace of the (improved) energy-momentum tensor $\theta_{\mu\nu}$, and has the limit $4 > d_\theta > 2$ (Ref. 10) from the positivity properties of anomalous dimensions. Using CEA and SPEAR data,[14–17] Nachtmann obtained a fit with the following values of parameters:

$$R_\infty = 9, \quad B = 12, \quad \frac{4-d_\theta}{2} = 0.4 . \tag{3.2}$$

In order to extrapolate Eq. (3.1) to the present R data, with Ψ and Υ thresholds at $\sqrt{s_{0\Psi}} = 3.1$ GeV and $\sqrt{S_{0\Upsilon}} = 9.1$ GeV, respectively, we assume the validity of the following simple form:

$$R = \left[R^{\mathrm{I}}_\infty - \frac{B^{\mathrm{I}}}{s^{(4-d_\theta)/2}} \right] \theta(s_{0\Psi} - s) + \theta(s - s_{0\Psi})\theta(s_{0\Upsilon} - s) \left[R^{\mathrm{II}}_\infty - \frac{B^{\mathrm{II}}}{s^{(4-d_\theta)/2}} \right] + \theta(s - s_{0\Upsilon}) \left[R^{\mathrm{III}}_\infty - \frac{B^{\mathrm{III}}}{s^{(4-d_\theta)/2}} \right] . \tag{3.3}$$

We note the R_∞'s might deviate in general from the naive values of $R_\infty = 3\sum Q_i^2$ in a fixed-point theory[20] and hence they need not add up. Nor does the theory give an explicit relationship among them. Such anomalous behavior of the R_∞'s may presumably be related to the production mechanism of resonances and thresholds in a fixed-point theory, which are yet to be understood completely.

Taking experimental input[1,18] as

$$\begin{aligned} &R(s_1) = 2.1 \pm 0.2 \text{ at } \sqrt{s_1} = 2.2 \text{ GeV} , \\ &R(s_2) = 2.35 \pm 0.15 \text{ at } \sqrt{s_2} = 2.95 \text{ GeV} , \\ &R(s_3) = 3.25 \pm 0.3 \text{ at } \sqrt{s_3} = 4.23 \text{ GeV} , \\ &R(s_4) = 4.3 \pm 1.5 \text{ at } \sqrt{s_4} = 7 \text{ GeV} , \\ &R(s_5) = 4.0 \pm 0.5 \text{ at } \sqrt{s_5} = 12 \text{ GeV} , \\ &R(s_6) = 4.2 \pm 0.6 \text{ at } \sqrt{s_6} = 17 \text{ GeV} , \end{aligned} \tag{3.4}$$

we obtain

$$\begin{aligned} &R^{\mathrm{I}}_\infty = 3.61 \pm 0.23, \quad B^{\mathrm{I}} = 2.5 \pm 0.45 , \\ &R^{\mathrm{II}}_\infty = 6.97 \pm 1.05, \quad B^{\mathrm{II}} = 9.54 \pm 1.45 , \\ &R^{\mathrm{III}}_\infty = 5.02 \pm 1.0, \quad B^{\mathrm{III}} = 5.0 \pm 2.5 \end{aligned} \tag{3.5}$$

with[21]

$$\frac{4-d_\theta}{2} = 0.32 . \tag{3.6}$$

Using Eqs. (3.5) and (3.6) in Eq. (3.3) we observe that a fixed-point theory gives the following phenomenological asymptotic limit of R:

$$R_\infty = 5.02 \pm 1.0 . \tag{3.7}$$

Using Eqs. (3.5) and (3.6), we find that 90% and 99% saturations of R_∞ are reached at the c.m. energy $\sqrt{s_\infty}$ given by

$$\sqrt{s_\infty} = 36 \text{ GeV} \tag{3.8}$$

and

$$\sqrt{s_\infty} = 1308 \text{ GeV} , \tag{3.9}$$

respectively. Equations (3.8) and (3.9) are to be compared with Nachtmann's[10] 90% and 99% saturation points of

$$\sqrt{s_\infty} \approx 35 \text{ GeV} \tag{3.10}$$

and

$$\sqrt{s_\infty} \approx 453 \text{ GeV} , \tag{3.11}$$

respectively. In Fig. 5, we show our prediction with a fixed-point theory, Eq. (3.3), which is consistent with data.

IV. CONCLUSIONS

In this paper, we have addressed ourselves to the R problem within the frameworks of a free-field

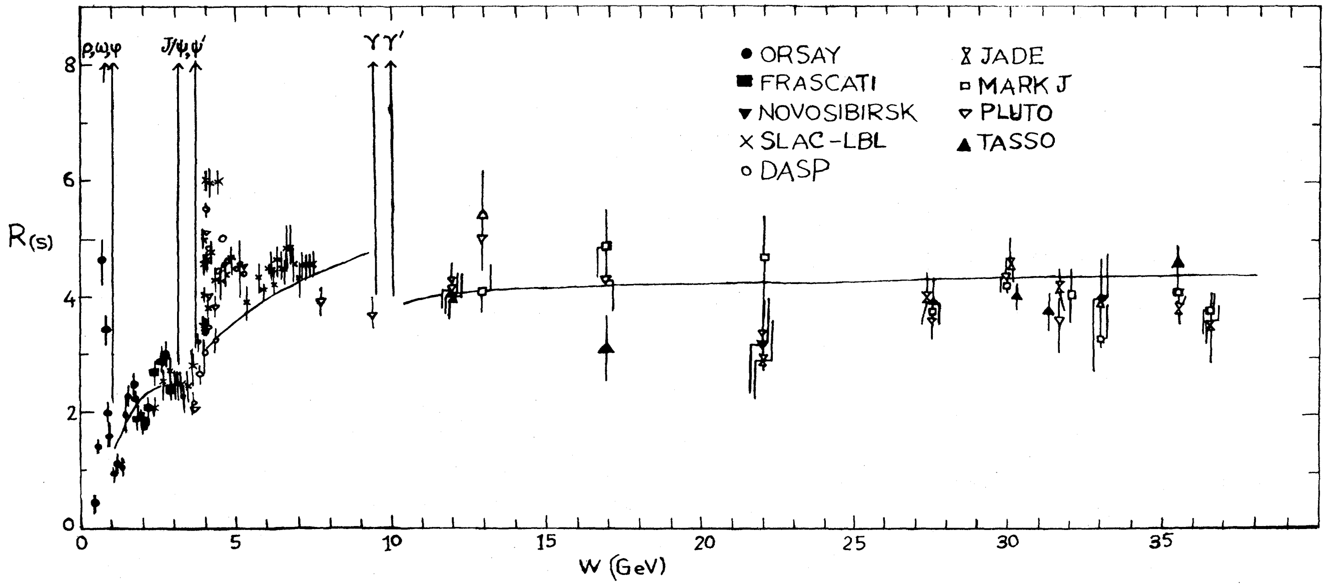

FIG. 5. $R(s)$ vs W in a fixed-point theory.

theory and a field theory with an infrared-stable fixed point. Present data on R do not rule out either of these two models. Our result thus suggests that both of them survive as alternatives to standard QCD as far as the present data on R are concerned. Future experiments can alone determine whether these alternative models can survive in R data even at higher energies.

ACKNOWLEDGMENTS

Both of the authors are grateful to Professor G. Wolf of DESY, West Germany, for assisting us with recent data on electron-positron physics while one of them (A.K.M.) acknowledges financial support from the University Grants Commission (India).

[1]For a recent review, see K. H. Mess and B. H. Wilk, Report No. DESY 82-011, 1982 (unpublished).

[2]A. Zee, Phys. Rev. D 8, 4038 (1973).

[3]T. Appelquist and H. Georgi, Phys. Rev. D 8, 4000 (1973).

[4]T. Appelquist and H. D. Politzer, Phys. Rev. D 12, 1404 (1975).

[5]E. C. Poggio, H. R. Quinn, and S. Weinberg, Phys. Rev. D 13, 1958 (1976).

[6]R. Shankar, Phys. Rev. D 15, 755 (1979).

[7]R. M. Barnett, M. Dine, and L. McLerran, Phys. Rev. D 22, 594 (1980).

[8]D. K. Choudhury, Nuovo Cimento 28A, 510 (1975).

[9]D. K. Choudhury, Nuovo Cimento 31A, 669 (1976).

[10]O. Nachtmann, Phys. Lett. 51B, 469 (1974).

[11]T. E. Augustin *et al.*, Phys. Rev. Lett. 33, 1406 (1974).

[12]C. Bacci *et al.*, Phys. Rev. Lett. 33, A649 (1974).

[13]G. S. Abrams *et al.*, Phys. Rev. Lett. 33, 1453 (1974).

[14]G. Tarnopolsky *et al.*, Phys. Rev. Lett. 32, 432 (1974).

[15]A. Litke *et al.*, Phys. Rev. Lett. 30, 1189 (1973).

[16]B. Bartoli *et al.*, Phys. Rev. D 6, 2374 (1972).

[17]M. Grilli *et al.*, Nuovo Cimento 13A, 593 (1973).

[18]TASSO Collaboration, Report No. 79/74, 1979 (unpublished).

[19]K. G. Wilson and J. Kogut, Phys. Rev. 12, 75 (1974).

[20]S. S. Shei and T. M. Yan, Phys. Rev. D 8, 2457 (1973).

[21]In our numerical analysis we find a fairly good fit even with $(4-d_\theta)/2=0.84$, 0.71, 0.61, 0.5, and 0.4 besides with 0.32. We choose the solution (3.6) assuming that the dimension of θ, the trace of the energy-momentum tensor, is near 4 in conformity with the conjecture in Ref. 10.